Article

Performance of Catalytic Fast Pyrolysis Using a γ-Al₂O₃ Catalyst with Compound Modification of ZrO₂ and CeO₂

Zeyu Xue[ID]**, Zhaoping Zhong *, Bo Zhang * and Chao Xu**

Key Laboratory of Energy Thermal Conversion and Control of Ministry of Education, Southeast University, Nanjing 210096, China; jszyxue@163.com (Z.X.); jiangchaonine@gmail.com (C.X.)

* Correspondence: zzhong@seu.edu.cn (Z.Z.); bozhang@seu.edu.cn (B.Z.); Tel.: +86-025-83794700 (Z.Z.)

Abstract: To investigate the catalytic pyrolysis performance of complex metal oxide catalysts for biomass, γ-Al₂O₃ was prepared through the precipitation method, and then ZrO₂ and γ-Al₂O₃ were blended in the proportion of 2:8 using the co-precipitation method. Next, CeO₂ was loaded on the surface of the catalyst for further modification. The three catalysts, A, ZA and CZA, were obtained. The specific surface and acidity of the catalysts were characterized by nitrogen adsorption–desorption and NH₃-Temperature Programmed Desorption (NH₃-TPD) respectively. The catalytic pyrolysis performance of catalysts for bamboo residues was investigated by Pyrolysis gas chromatography mass spectrometry (Py-GC/MS). Chromatograms were analyzed for identification of the pyrolysis products and the relative amounts of each component were calculated. Experimental results indicated that catalyst A had a good catalytic activity for the fast pyrolysis of bamboo residues. The addition of ZrO₂ and CeO₂ could continuously enhance the acidity of the catalyst and further promote the pyrolysis of macromolecular compounds and deoxidation of oxygen-containing compounds. Finally, catalyst CZA, obtained by compound modification, could not only dramatically reduce the relative content of phenol, acid and aldehyde and other oxygen-containing compounds, but also achieved the maximum hydrocarbon yield of 23.38%. The catalytic performance of catalyst CZA improved significantly compared with catalyst A.

Keywords: biomass; pyrolysis; catalytic cracking; Py-GC/MS; complex metal oxides

1. Introduction

Catalytic fast pyrolysis of biomass is one of the most effective ways to convert biomass into high grade bio-oil, and it is particularly essential to select excellent catalysts [1–4]. In previous studies, researchers conducted a large number of experimental studies using zeolite catalysts. Among them, the most efficient zeolite is HZSM-5 due to its shape selectivity and aromatization for aromatic petrochemical hydrocarbons [5–7]. Although it can significantly increase the hydrocarbon content in bio-oil and has excellent catalytic properties, the microporous structure and strong surface acidity of HZM-5 make it difficult for large-scale oxygenates to enter the pores. Meanwhile, the surface of HZSM-5 is susceptible to coking [8–10].

It is now widely accepted that mesoporous materials have been the most promising catalysts for the catalytic pyrolysis of biomass [11,12]. Its large pore size provides sufficient mass transfer channels for reactants and products, and avoids blockage of the pores. Lu found that using ZrO₂, TiO₂, and a combination of both as catalyst carriers could effectively reduce the yield of phenols, acids and carbohydrates, while increasing the yield of hydrocarbons [13]. Among them, the combination had the best catalytic effect but its yield of aromatics was as low as 13% due to the small specific surface

area. Mochizuki conducted an experimental study using SiO_2 as a catalyst with a higher specific surface area [9]. He found that the SiO_2 catalyst could significantly reduce the content of oxygenated compounds in bio-oil and improved hydrocarbon yield to 14.3%. Although the SiO_2 catalyst had a higher surface area, its weaker acidity limited hydrocarbon yield. Therefore, it is necessary to develop a catalyst with a larger specific surface area and stronger acidity.

Because of the large specific surface area and low cost, γ-Al_2O_3 is a widely used catalyst in industry [14–16]. On the other hand, ZrO_2 is a material with good thermal stability, and was also reported to be the only metallic oxide to have both surface acid sites and basic sites [17]. ZrO_2 has been widely used in the field of catalysis, but sometimes its application is limited due to its small specific surface area and poor mechanical strength [18]. Accordingly, the combination of ZrO_2 and γ-Al_2O_3 as composite catalysts not only has a large specific surface area, good thermal stability and suitable pore size distribution from γ-Al_2O_3, it can also fully exert the advantages of ZrO_2, which is beneficial to the dispersion of active components and the improvement of catalytic activity. Although ZrO_2 and γ-Al_2O_3 composite catalysts have received extensive attention [19–21], they have not been report in the field of catalytic pyrolysis yet. In this study, a ZrO_2 and γ-Al_2O_3 catalyst was prepared to study its catalytic pyrolysis performance. Additionally, CeO_2 can promote the redox ability of the metal, and the surface pores of the CeO_2 can easily store and supply oxygen [22,23]. In order to further increase the catalytic activity of the ZrO_2 and γ-Al_2O_3 catalyst, its surface was loaded with CeO_2 as an active component to improve the performance of the catalyst.

2. Results and Discussion

2.1. Characteristics of the Catalysts

2.1.1. Characterization of the Adsorption–Desorption of N_2

The specific surface area, pore volume, and pore width of the catalysts are shown in Table 1. The pore width of the three catalysts ranged from 2 to 50 nm. The adsorption isotherms of the three catalysts showed obvious hysteresis loops, indicating that the catalysts were mesoporous materials. As can be seen from the table, when incorporated with ZrO_2, the specific surface area of the catalyst was increased. The specific surface area of the catalyst decreased with CeO_2 loading on the ZA surface as CeO_2 entered into the pores of the carrier. In addition, with the loading of CeO_2, the average pore size of the catalyst increased. After loading of CeO_2, some pores may become blocked, thus resulting in the increase in the average pore width.

Table 1. Specific surface area, pore volume and aperture of the catalysts.

Catalyst	Specific Surface Area (m^2/g)	Pore Volume (cm^3/g)	Average Pore Width (nm)
A	162.1	0.45	11.17
ZA	206.8	0.52	10.09
CZA	177.1	0.54	12.12

2.1.2. Characterization of NH_3-TPD

Figure 1 shows the NH_3-TPD curves of the three catalysts prepared in this study. The temperature ranges of weak, medium, and strong acids were defined as 100–300 °C, 300–500 °C, and 500–700 °C, corresponding to low temperature, medium temperature and high temperature desorption peaks, respectively. Judging from the height and location of the desorption peak, catalyst A had a significant low temperature and high temperature desorption peak at 100 °C and 600 °C, respectively. When ZrO_2 was incorporated into catalyst A, the low temperature desorption peak offset to the right with the increase of acidity. The desorption peak at the high temperature significantly rose, and strong acid sites increased accordingly. When CeO_2 was further loaded on the surface of catalyst ZA, the weak acid sites of catalyst CZA decreased significantly, and the weak acidity was impaired. The high temperature

desorption peak increased again, and the strong acid sites increased as well. It could be concluded that the blending of ZrO_2 and the loading of CeO_2 gradually enhanced the strong acidity of catalyst A.
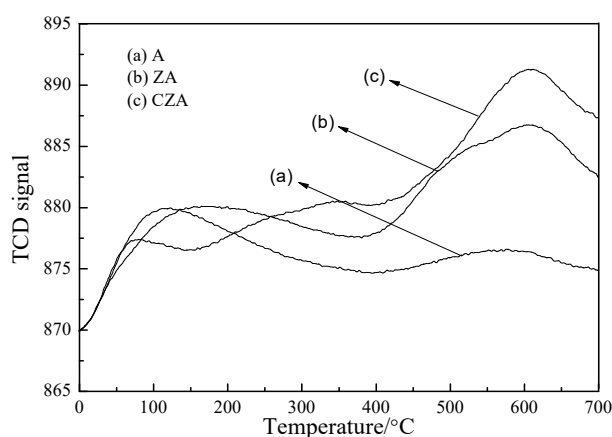

Figure 1. NH_3-TPD curves of the catalysts.

2.2. Effect of the Catalyst on Pyrolysis

The chromatographic peak area of each component of the released volatiles is generally considered to be proportional to the product amount, thus the peak area percentage of the product is proportional to its relative content [24]. In each experiment, the quality of the bamboo powder was kept constant. Therefore, the distribution of the chromatographic peak area of the product in the different chromatograms could reflect the change in the relative content of the product in volatile products. This semi-quantitative method was often used to calculate the relative content of different components in volatile products [25,26].

During catalytic pyrolysis, the presence of the catalyst could cause the volatile products to crack into small molecules or polymerize into chars, which reduced the yield of bio-oil. In order to evaluate the influence of the catalyst on the total yield of the volatile product, the total peak areas in different chromatograms were compared in this study. The total peak area was divided into two parts: the CO and CO_2 peak area and the volatile organics peak area. Their relative amount distribution is shown in Figure 2. It could be seen that after being modified by ZrO_2 and further loaded with CeO_2, the relative amount of volatile organics gradually decreased, while the amount of CO and CO_2 gradually increased, which indicated that the catalytic activity of catalyst A was improved by ZrO_2 and CeO_2, and its catalytic deoxygenation performance was also enhanced, cracking oxygenated compounds into small molecular gases.
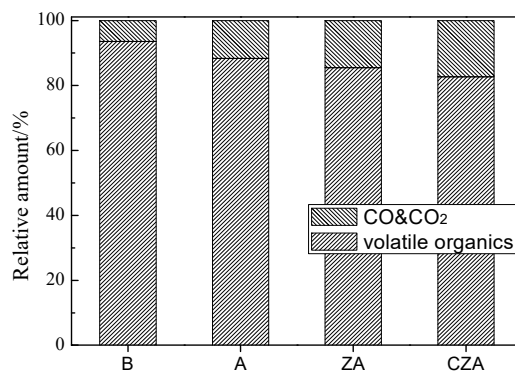

Figure 2. Relative content of CO and CO_2 and volatile organics by the effect of different catalysts.

2.2.1. Effect of Catalyst on the Relative Content of Pyrolysis Products

Figure 3 shows the chromatograms of the products before and after the use of catalyst. In this study, products with large chromatographic peak areas were marked in the form of a structural formula. It could be observed that with the participation of catalysts, components such as phenols and benzofuran with higher relative contents in the non-catalytic pyrolysis products reduced to different degrees. Some of these compounds may have only undergone ring-opening reactions. However combined with the decrease of the peak area of CO and CO_2, it could be inferred that deoxygenation reactions such as decarbonylation, decarboxylation and dehydroxylation took place among the other components. It was observed that hydroxyacetone produced by non-catalytic pyrolysis underwent the effect of cracking and dehydroxylation reactions and was transferred into butane under the influence of catalyst A, ZA and CZA, respectively. The corresponding possible reaction equation is shown as follows:
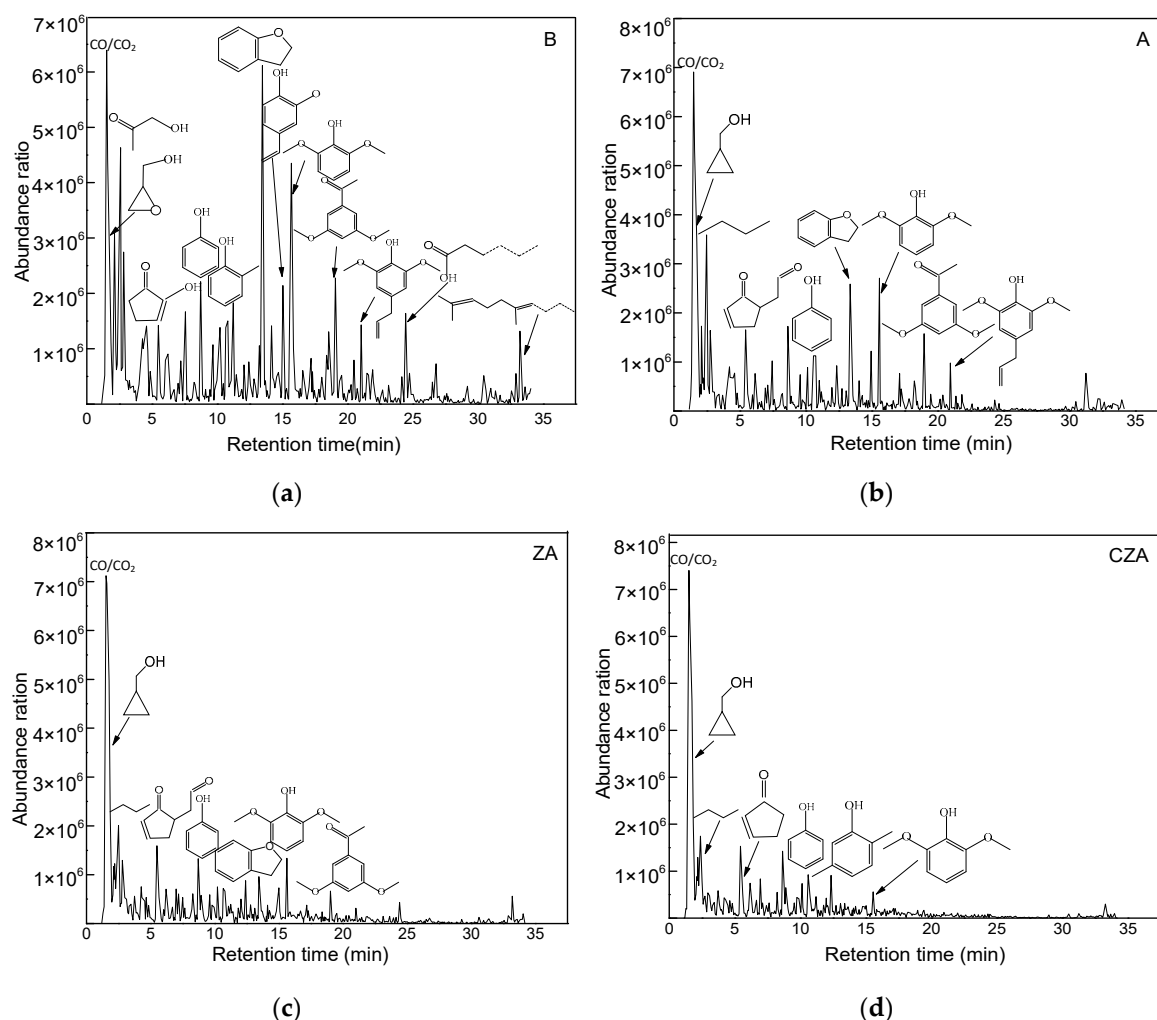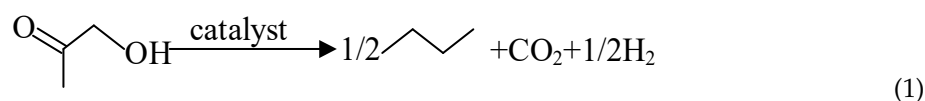
$$\text{hydroxyacetone} \xrightarrow{\text{catalyst}} 1/2 \text{ butane} + CO_2 + 1/2H_2 \tag{1}$$

Figure 3. GC/MS Chromatogram of the pyrolysis products: (**a**) without catalyst, (**b**) with catalyst A, (**c**) with catalyst ZA, (**d**) with catalyst CZA.

In addition, it could be seen that a certain amount of macromolecular compounds such as long-chain fatty acids and long-chain aliphatic hydrocarbons were produced in pyrolysis in the absence

of catalyst. However, with the participation of catalyst, especially for catalyst CZA, the high molecular weight compounds basically disappeared.

The volatile organic compounds were divided into nine groups in this study: phenols, alcohols, hydrocarbons, ketones, acids, furans, aldehydes, esters and others. As shown in Figure 4, when no catalyst was involved in pyrolysis, the relative contents of phenols, acids and aldehydes in the pyrolysis products were 29.56%, 11.25% and 7.37%, respectively. These compounds could decrease the combustion performance and stability of the pyrolysis oil. In contrast, the relative contents of beneficial components such as alcohols, ketones, furans, and esters were 7.09%, 24.89%, 9%, and 6.66%, respectively. Furthermore, the relative content of the hydrocarbons, the most desirable compound in pyrolysis products, only accounted for 3.15% in the product. However, in catalytic pyrolysis, the relative contents of phenols, ketones, acids, furans, aldehydes and esters declined to varying degrees. It was mainly because the deoxidization reactions, such as the dehydroxylation, decarbonylation, decarboxylation and cracking reactions, took place in pyrolysis. At the same time, the relative content of alcohols and hydrocarbons increased after being modified by ZrO_2 and further loaded with CeO_2.
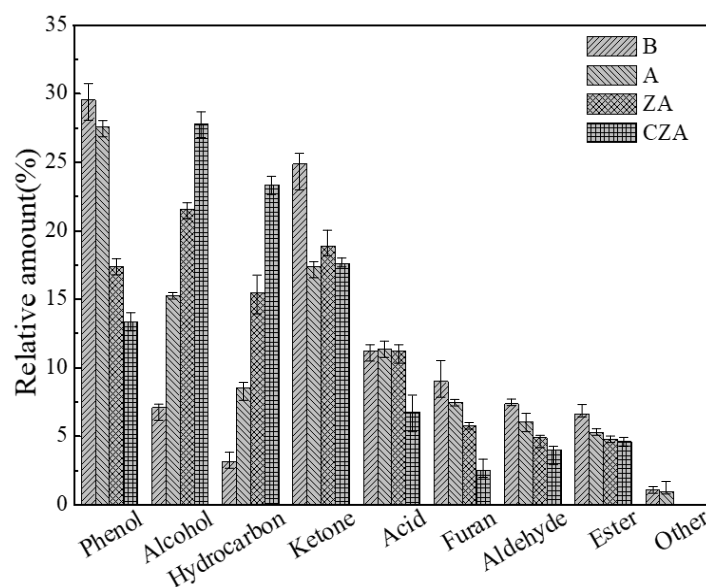

Figure 4. Change in relative amount of pyrolysis products.

In this study, catalysts could reduce the relative content of unfavorable components such as phenols, acids and aldehydes. Meanwhile the relative content of hydrocarbons also increased through a series of deoxygenation. Judging from the two aspects above, catalyst A had a good catalytic pyrolysis performance. It could be seen that after modification, the deoxidation and cracking performances of catalyst A were greatly improved, and its catalytic pyrolysis performance was further promoted.

Particularly, under the effect of catalysts, phenols in the product could be transformed into other compounds through three pathways as shown in Figure 5. In reaction A, in addition to the cleavage of methylene bridges and methylene oxy bridges of benzene rings, the heavy phenols (phenol compounds with a large carbon number) also transformed into light phenols, which contain functional groups such as methoxy [27]. In reaction B, the phenolic compounds transformed into aromatic hydrocarbons through deoxidation reactions such as dehydroxylation [28]. Furthermore, ring-opening reactions may occur and convert aromatic hydrocarbons into aliphatic hydrocarbons, which coincide with the significant increase in the content of hydrocarbons after the use of catalysts. In reaction C, phenolic compounds underwent ring-opening reactions and formed alcohol compounds with the retention of hydroxyl [29,30]. This could be proved by the increase in the relative content of alcohols.
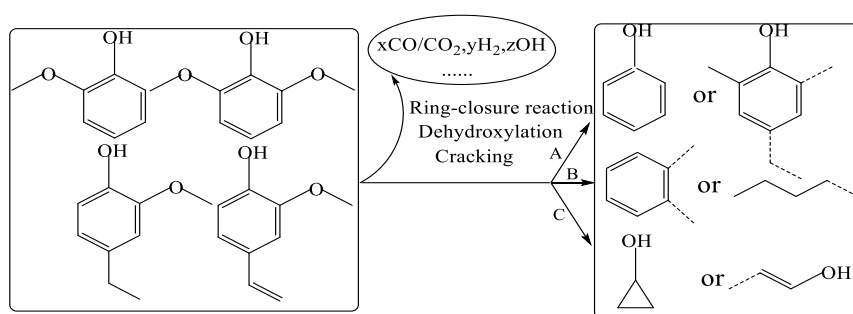
Figure 5. Possible transfer pathways of phenol.

With the participation of catalyst A, reaction A in Figure 5 may take place; thus, the relative content of phenolic compounds did not change significantly. However, the relative content of phenolic compounds reduced significantly with the participation of catalyst ZA and CZA. Meanwhile, the relative contents of alcohol and hydrocarbon compounds increased remarkably, which indicated that the reaction B and C dominated, and the deoxygenation and cracking performance of the catalysts were both improved.

2.2.2. Catalytic Effect on Distribution of Pyrolysis Products

Catalytic Effect on Phenols

The relative content of phenols was highest in the products of bamboo fast pyrolysis. In this study, phenolic compounds were divided into nine groups as shown in Figure 6. Under the effect of catalyst A, the relative content of heavy phenolic compounds such as benzenetriol, methoxyphenol, 2,6-dimethoxyphenol, 2-methoxy-4-vinylphenol, 2-methoxy-4-methylphenol and 4-ethyl-2-methoxyphenol decreased significantly, while the relative content of phenol, dimethylphenol and ethylphenol increased, indicating that phenols were mainly formed through reaction A under the effect of the catalyst A. In the case of catalyst ZA, the total relative content of heavy phenols decreased. To be specific, 2-methoxy-4-methylphenol and 4-ethyl-2-methoxyphenol were not detected, while the relative content of phenol increased significantly. However, the content of xylenol also decreased remarkably, indicating that methyl was removed from xylenol immediately after its transformation from heavy phenols. Therefore, the phenols were involved in reaction A in Figure 5 under the effect of catalyst ZA.
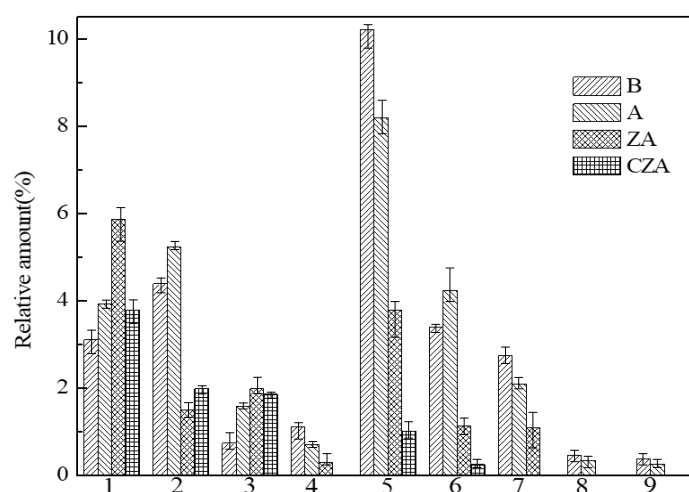

Figure 6. Phenol compounds distribution as a function of catalysts. 1. Phenol, 2. Xylenol, 3. Ethyl phenol, 4. Benzenetriol, 5. Syringol, 6. Metoxyphenol, 7. Vinyl-methoxy phenol, 8. Methyl methoxyphenol, 9. Ethyl methoxyphenol.

In the case of catalyst CZA, the total relative content of heavy phenols obviously decreased, and three kinds of heavy phenols were not detected in the product. Meanwhile, the relative content of phenol increased very little compared with the case of catalyst ZA, indicating that whenreaction A occurred, the degree of reaction B and C increased simultaneously coinciding with an increased contribution of reaction B and C. In these reactions, phenols could convert into alcohols by opening the benzene ring or transforming into hydrocarbons by deoxygenation.

Catalytic Effect on Acids

Two kinds of acids: acetic acid and long chain fatty acids were obtained in the fast pyrolysis of bamboo powder. The presence of acids could adversely affect the properties of bio-oils and produce persistent corrosive effects on metals such as aluminum, brass, and carbon steels during its utilization [31,32]. In addition, acids can also promote the aldol reaction and accelerated the aging of bio-oils [33].

Of all ester compounds, only methyl acetate was detected in this research. In order to simplify the analysis, methyl acetate was also classified into acid compounds. As shown in Figure 7, compared with non-catalytic pyrolysis, the relative contents of methyl acetate and long-chain fatty acids decreased while the relative content of acetic acid increased under the effect of catalysts A and ZA. The main reason may be that when the decarboxylation reaction of acids occurred, acetic acid was produced by a cracking reaction of methyl acetate and long-chain fatty acids. In the case of catalyst CZA, the contents of acetic acid, methyl acetate and long-chain fatty acids all decreased, indicating that decarboxylation occurred to acetic acid subsequently after its transformation from methyl acetate and long-chain fatty acids. It could be concluded that after the loading of CeO_2 on catalyst ZA, the decarboxylation ability was enhanced. In the previous experimental studies conducted in Py-GC/MS, the use of mesoporous catalysts increased the relative content of acids in the products [26,34,35]. Therefore, the catalytic cracking ability of catalyst CZA to acids was slightly superior to these mesoporous catalysts, and it could greatly improve the quality of bio-oils.
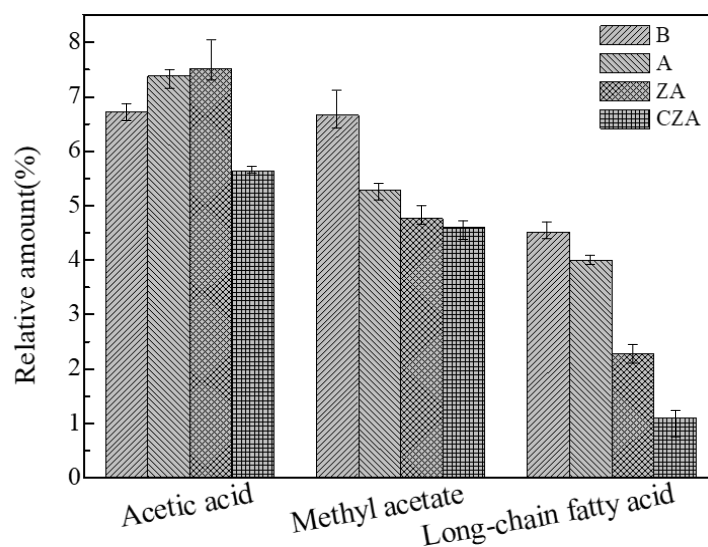

Figure 7. Effects of the catalysts on the acid compounds.

Catalytic Effect on Ketones

In the process of fast pyrolysis, the pyrolytic ring opening of hemicellulose and cellulose formed various low molecular weight products with carbonyl compounds as major products [36]. As shown in Figure 8, in this study, ketone compounds obtained by pyrolysis were divided into six groups, namely, acetone, butanone, pentanedione, cyclopentenone, methoxyacetophenone and others.
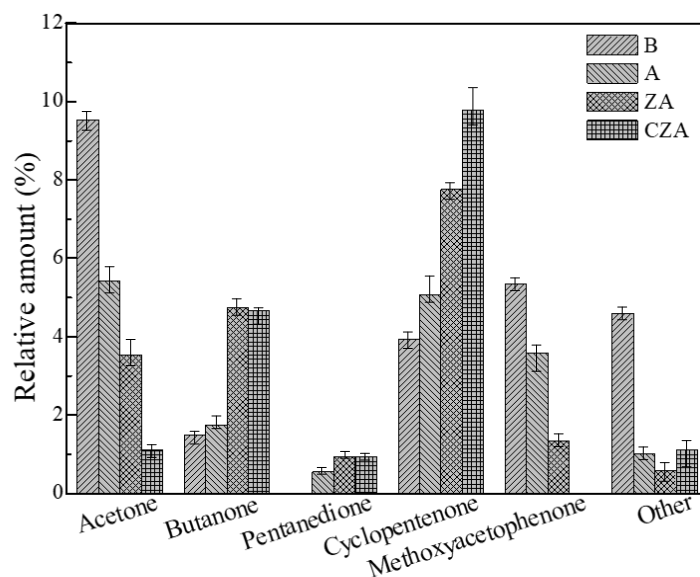
Figure 8. Effects of the catalysts on the ketone compounds.

Compared with non-catalytic pyrolysis, in the case of catalyst A, ZA and CZA, the relative contents of acetone, methoxyacetophenone and other compounds such as hexanone decreased. However, the relative contents of butanone, pentanedione and cyclopentenone increased significantly. Based on the fact that the total relative content of ketone compounds decreased after the use of the catalyst, it could be inferred that the decarbonylation reaction occurred in part of the ketone compounds, meanwhile butanone, pentanedione and cyclopentenone were produced under the effect of the catalyst. Taking the transformation from acetone to cyclopentenone as an example, the following reaction is proposed:

$$2C_3H_6O \xrightarrow{catalyst} C_5H_6O + CO + 3H_2 \tag{2}$$

Based on the above analysis, the catalytic effect of the three catalysts used in this study on ketones was not very desirable. This was probably because the C and O atom in the carbonyl compounds were linked by a double bond, which was firm and difficult to break. Considering the amount of catalysts added and the residence time of pyrolysis gas in the catalyst layer, the decarbonylation reaction did not occur completely before the pyrolysis gas entered GC/MS.

Catalytic Effects on Furans

Previous studies have confirmed that furan compounds are the dehydration products of carbohydrates [37,38]. In this study, in non-catalytic fast pyrolysis products, only benzofuran was detected. The catalytic effect of the catalysts on benzofuran is shown in Figure 9.

Under the effect of catalyst ZA, the relative content of benzofuran reduced sharply while the relative contents of methylfuran and furan both increased significantly. Analysis of the material balance of furan compounds showed that the cracking reaction of the five-membered heterocycle and benzene ring took place simultaneously in part of benzofuran, which led to the formation of small molecule compounds. Meanwhile, the cracking reaction took place in the benzene ring in the other part of benzofuran, generating methylfuran and furan. In the case of catalyst CZA, the relative content of benzofuran reduced to 1.04%, meanwhile the contents of methyl furan and furan were as low as 0.32% and 1.18%, respectively. This indicated that benzofuran mainly underwent the cracking reaction of the five-membered heterocycle and benzene ring. It could be seen that the catalytic cracking performance of the catalyst CZA was significantly improved compared with catalyst A and ZA.
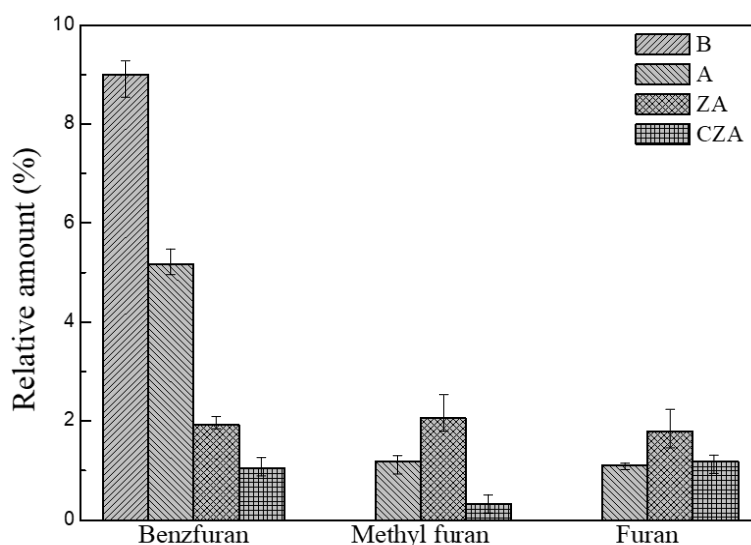
Figure 9. Effects of the catalysts on the furan compounds.

Catalytic Effect on Hydrocarbons

Hydrocarbons increase the heat value of bio-oil and is regarded as the most favorable component in bio-oil. The relative content of hydrocarbons in biomass catalytic pyrolysis products is also an important indicator to evaluate the catalyst performance. The effect of the catalysts on the distribution of hydrocarbon compounds is shown in Figure 10.
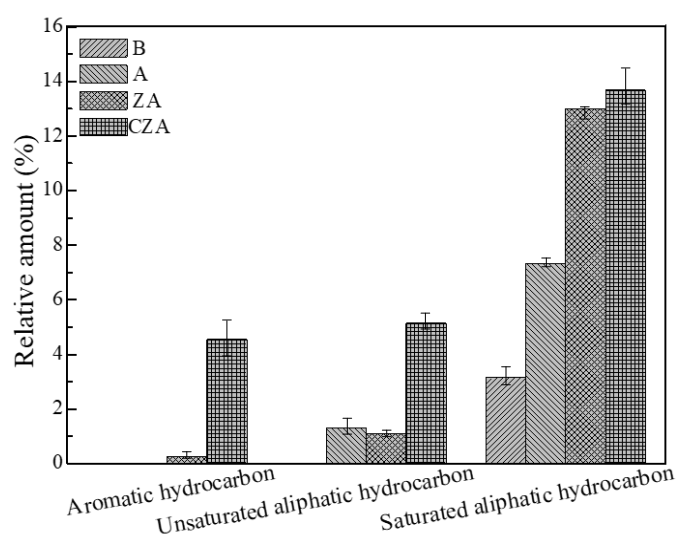

**Figure 10.** Effects of the catalysts on the hydrocarbon compounds.

In this study, saturated aliphatic hydrocarbons only accounted for 3.15% in the non-catalytic pyrolysis product. However, under the effect of catalyst A, the relative content of saturated aliphatic hydrocarbons increased to 7.34%, and a small amount of unsaturated aliphatic hydrocarbons was detected. After being modified by ZrO_2, the relative content of saturated aliphatic hydrocarbons increased from 7.34% to 13%, and 0.27% content of aromatic hydrocarbons was detected at the same time, which indicated that the catalyst ZA had limited aromatization properties. After the CeO_2 was further loaded on the surface of catalyst ZA, the relative content of saturated aliphatic hydrocarbons increased slightly, but the relative contents of unsaturated aliphatic hydrocarbons and aromatic hydrocarbons increased from 1.1% and 0.27% to 5.15% and 4.55%, respectively, which indicated that

the catalytic cracking and aromatization performance of catalyst CZA were significantly improved compared with catalyst ZA.

Catalytic Effect on Other Compounds

The non-catalytic fast pyrolysis of bamboo powder produced six kinds of aldehyde compounds such as acetaldehyde, succinaldehyde and furfural, and the total relative content reached 7.37%. With the participation of catalysts, the total relative content of aldehyde compounds decreased. Meanwhile, as a result, the number of aldehyde species also reduced correspondingly. Under the effect of catalyst CZA, only 3-cyclopentene-1-acetaldehyde was detected, and the relative content of aldehydes reached its minimum of 3.99%.

Among the non-catalytic pyrolysis products of bamboo powder, only glycidol was detected as an alcohol compound, and its relative content was 7.09%. However, cyclopropanemethanol dominated the alcohol species after the introduction of catalyst A, ZA and CZA. Its relative content constantly increased with the addition of ZrO_2 and the loading of CeO_2, which reached 11.38%, 16.66%, and 18.47%, respectively. On one hand, cyclopropanemethanol may be generated in the reaction of glycidol and olefin in the hydrocarbon pool under the effect of the catalyst. The possible reaction equation is as follows:

$$1/2 C_3H_6 + \text{glycidol} \xrightarrow{\text{catalyst}} \text{cyclopropanemethanol} + 1/2 CO_2 + 1/2 H_2 \tag{3}$$
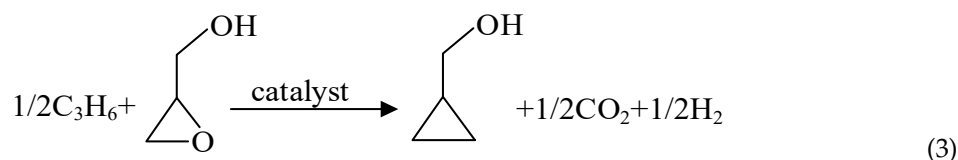
On the other hand, combined with the substantial decrease of relative content of phenolic compounds, the cracking reaction of the benzene ring probably occurred in phenolic compounds under the effect of catalysts, and then the ring-closing reaction occurred.

Ether and pyran compounds were also detected in non-catalytic pyrolysis products of bamboo powder. However, because of their low content and because they vanish in catalytic pyrolysis, they were neglected in this research.

3. Experimental

3.1. Materials

The biomass used for catalytic pyrolysis in the experiments was bamboo residue (B) from Huzhou, Zhejiang Province in China. The bamboo powder with a particle size of 100 meshes was prepared by crushing and sieving before experiment. Its ultimate analysis is shown in Table 2.

Table 2. Ultimate analysis of bamboo residual, %.

Ultimate Analysis	C	H	O	N	S
Bamboo residue	51.51	6.12	42.05	0.21	0.11

3.2. Preparation of Catalysts

Firstly, 10% (v/v) ammonia solution was dropwise added into an aqueous solution of aluminum nitrate nonahydrate (AR, Aladdin, Shanghai, China) to adjust the pH between 9 and 10. After aging for 5 h, the solution was filtered using a vacuum pump and a Buchner funnel, then the precipitate was washed by ultrapure water to bring the pH to about 7. After it was dried in an oven at 110 °C for 10 h, it was finally placed in a muffle furnace to be calcined at 500 °C for 4 h. Thus, the γ-Al_2O_3 catalyst (A) was obtained.

Secondly, 29.42 g of aluminum nitrate nonahydrate (AR, Aladdin) and 3.49 g of zirconium nitrate pentahydrate (AR, Aladdin) were dissolved in ultrapure water, and ammonia solution was added

to make pH between 9 and 10 during stirring. Then the precipitate was filtered, washed, dried and calcined at 500 °C for 4 h in a muffle furnace. Thus, the ZrO_2 and γ-Al_2O_3 catalyst (ZA) with mass ratio of 2:8 was obtained.

Finally, 2.02 g of cerium nitrate hexahydrate (AR, Aladdin) was dissolved in ultrapure water, 10 g of ZA was added and stirred for 2 h. After it was dried at 110 °C for 10 h, the precipitate was lastly calcined at 500 °C for 4 h to obtain the CeO_2/ZrO_2 and γ-Al_2O_3 catalyst (CZA) with a loading of 8 wt%.

In this study, the three catalysts for the catalytic pyrolysis of bamboo powder were prepared by precipitation, co-precipitation and the dipping method, respectively. After grinding, and sieving, the catalyst with a particle size of about 100 meshes was obtained.

3.3. Characterization of the Catalysts

Adsorption–desorption of N_2 was performed using an ASAP 2400 adsorption apparatus (Micromeritics, Norcross, GA, USA). The specific surface area was calculated using the BET method, and the micropore volume was calculated by the t-plot method.

To determine the surface acidity of the samples, the NH_3-TPD experiment was carried out using a 3010 chemisorption instrument (Finetec, Quzhou, China). In the experiment, about 0.1 g of the sample was weighted and helium was used as a carrier gas at 10 mL/min. It was pretreated at 400 °C for 0.5 h. When cooled to 80 °C, a 5% NH_3/N_2 flow at 10 mL/min was used, while the temperature was increased to 700 °C at 10 °C/min. In the test, desorption of NH_3 was detected by a thermal conductivity detector (TCD).

3.4. Experimental Methods

3.4.1. Catalytic Pyrolysis Experimental Apparatus and Method

Py-GC/MS (Lu et al., 2010; Wang et al., 2017; K.P. et al., 2014) was widely applied in the experimental analysis of biomass pyrolysis [13,39,40]. In this study, the pyrolysis experiment was conducted in a CDS-5200 Pyrolysis Instrument (CDS, Chester, PA, USA). The bamboo powder and catalyst were packed in a quartz tube with a diameter of 2 mm and a tube diameter of 20 mm, and the filling method is shown in Figure 11. In the quartz tube, the bamboo powder was constant at 1 mg and the catalysts on both sides were set as 1 mg too. Considering the carrier gas (99.999% pure helium) flowed unidirectionally at 1.0 mL/min, the mass ratio of catalyst to bamboo powder was 1:1. In the experiment, the platinum wire on the outside of the quartz tube rapidly rose to a test temperature of 600 °C at a heating rate of 20 °C/ms and was maintained for 20 s. Then, the pyrolysis gas was passed into the 7890A/5975C gas chromatograph/mass spectrometer (Agilent, Santa Clara, CA, USA) by high-purity helium gas. The HP-5MS (0.25 mm × 0.25 μm × 30 m) chromatographic column was used to separate the pyrolysis gas in the GC/MS system. The chromatographic column has been widely used in the detection of bio-oil components and can be used to separate the main components of bio-oil. High-purity helium was used as the carrier gas with a flow rate of 1 mL/min and a split ratio of 1:80. In this experiment, the temperature was maintained at 40 °C for 3 min, then increased to 180 °C at a rate of 5 °C/min, then maintained for 2 min, and finally increased to 280 °C at 10 °C/min. After the experiment, each substance in the pyrolysis gas could be identified by comparing it with the NIST MS database.

According to the optimum temperature of bamboo residue pyrolysis determined by the previous study [39,41,42], the pyrolysis temperature in this study was set as 600 °C. Bamboo powder was firstly pyrolyzed alone, and then pyrolyzed with the three catalysts respectively. The mass ratio of bamboo powder to catalysts was constant at 1:1. All the experiments were carried out three times under the same conditions to obtain the average value.
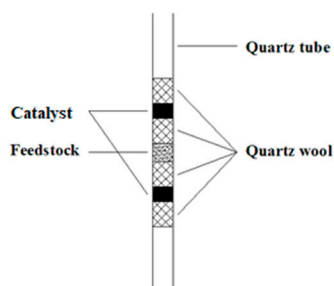
Figure 11. Diagram of quartz tube.

3.4.2. Calculation of Relative Content of Product Components

To analyze catalytic pyrolysis products, the relative content of each pyrolysis product (R_{yield}) was calculated by Equation (4):

$$R_{\text{yield}} = \frac{P_s}{P_{\text{total}} - \sum P_{\text{CO\&CO}_2}} \tag{4}$$

where P_s represents the peak area of the component in the pyrolysis product, P_{total} represents the total peak area of all products detected, and $P_{\text{CO\&CO2}}$ represents the peak area of CO and CO_2.

4. Conclusions

In this paper, the catalytic pyrolysis performance of catalysts A, ZA and CZA was investigated. By analyzing the chromatogram and changes in the relative contents of pyrolysis products, it was found that the presence of catalyst A could preliminarily promote the cracking of macromolecules and reduce the total relative content of unfavorable components such as phenols, acids, aldehydes and others by 3.20%, meanwhile coinciding with an increase in the relative content of hydrocarbons by 5.38%. In addition, with the blending of ZrO_2 and the loading of CeO_2, the catalytic cracking and catalytic deoxygenation performance was continually improved. Among the three catalysts, catalyst CZA exhibited the optimum performance and reduced the total relative content of unfavorable components such as phenols, acids, aldehydes and others by 24.09% and also increased the relative content of hydrocarbons by 20.23%. The catalyst CZA showed excellent performance for fast pyrolysis compared with existing mesoporous molecular sieve catalysts.

References

1. Neves, D.; Thunman, H.; Matos, A.; Tarelho, L.; Gomez-Barea, A. Characterization and prediction of biomass pyrolysis products. *Prog. Energy Combust. Sci.* **2011**, *37*, 611–630. [CrossRef]
2. Czernik, S.; Bridgwater, A.V. Overview of applications of biomass fast pyrolysis oil. *Energy Fuels* **2004**, *18*, 590–598. [CrossRef]
3. Liu, C.J.; Wang, H.M.; Karim, A.M.; Sun, J.M.; Wang, Y. Catalytic fast pyrolysis of lignocellulosic biomass. *Chem. Soc. Rev.* **2014**, *43*, 7594–7623. [CrossRef] [PubMed]
4. Zhang, B.; Zhong, Z.P.; Min, M.; Ding, K.; Xie, Q.L.; Ruan, R. Catalytic fast co-pyrolysis of biomass and food waste to produce aromatics: Analytical Py-GC/MS study. *Bioresour. Technol.* **2015**, *189*, 30–35. [CrossRef] [PubMed]
5. Zhang, Y.D.; Chen, P.; Lou, H. In situ catalytic conversion of biomass fast pyrolysis vapors on HZSM-5. *J. Energy Chem.* **2016**, *25*, 427–433. [CrossRef]

6.　Adjaye, J.D.; Katikaneni, S.P.R.; Bakhshi, N.N. Catalytic conversion of a biofuel to hydrocarbons: Effect of mixtures of HZSM-5 and silica-alumina catalysts on product distribution. *Fuel Process. Technol.* **1996**, *48*, 115–143. [CrossRef]

7.　Williams, P.T.; Horne, P.A. The influence of catalyst regeneration on the composition of zeolite-upgraded biomass pyrolysis oils. *Fuel* **1995**, *74*, 1839–1851. [CrossRef]

8.　Mihalcik, D.J.; Mullen, C.A.; Boateng, A.A. Screening acidic zeolites for catalytic fast pyrolysis of biomass and its components. *J. Anal. Appl. Pyrolysis* **2011**, *92*, 224–232. [CrossRef]

9.　Mochizuki, T.; Atong, D.; Chen, S.Y.; Toba, M.; Yoshimura, Y. Effect of SiO_2 pore size on catalytic fast pyrolysis of Jatropha, residues by using pyrolyzer-GC/MS. *Catal. Commun.* **2013**, *36*, 1–4. [CrossRef]

10.　Bjorgen, M.; Olsbye, U.; Kolboe, S. Coke precursor formation and zeolite deactivation: Mechanistic insights from hexamethylbenzene conversion. *J. Catal.* **2003**, *215*, 30–44. [CrossRef]

11.　Kelkar, S.; Saffron, C.M.; Li, Z.L.; Kim, S.S.; Pinnavaia, T.J.; Miller, D.J.; Kriegel, R. Aromatics from biomass pyrolysis vapour using a bifunctional mesoporous catalyst. *Green Chem.* **2014**, *16*, 803–812. [CrossRef]

12.　Ying, J.Y.; Mehnert, C.P.; Wong, M.S. Synthesis and applications of supramolecular-templated mesoporous materials. *Angew. Chem. Int. Ed.* **1999**, *38*, 56–77. [CrossRef]

13.　Lu, Q.; Zhansg, Y.; Tang, Z.; Li, W.Z.; Zhu, X.F. Catalytic upgrading of biomass fast pyrolysis vapors with titania and zirconia/titania based catalysts. *Fuel* **2010**, *89*, 2096–2103. [CrossRef]

14.　Loviat, F.; Czekaj, I.; Wambach, J.; Wokaun, A. Nickel deposition on γ-Al_2O_3 model catalysts: An experimental and theoretical investigation. *Surf. Sci.* **2009**, *603*, 2210–2217. [CrossRef]

15.　Krár, M.; Kovács, S.; Kalló, D.; Hancsok, J. Fuel purpose hydrotreating of sunflower oil on Co Mo/Al_2O_3 catalyst. *Bioresour. Technol.* **2010**, *101*, 9287–9293. [CrossRef] [PubMed]

16.　Zheng, Y.; Chen, D.Y.; Zhu, X.F. Aromatic hydrocarbon production by the online catalytic cracking of lignin fast pyrolysis vapors using Mo_2N/γ-Al_2O_3. *J. Anal. Appl. Pyrolysis* **2013**, *104*, 514–520. [CrossRef]

17.　Tanabea, K.; Yamaguchib, T. Acid-base bifunctional catalysis by ZrO_2 and its mixed oxides. *Catal. Today* **1994**, *20*, 185–197. [CrossRef]

18.　Rezaei, M.; Alavi, S.M.; Sahebdelfar, S.; Yan, Z.F.; Teunissen, H.; Jacobsen, J.H.; Sehested, J. Synthesis of pure tetragonal zirconium oxide with high surface area. *J. Mater. Sci.* **2007**, *42*, 1228–1237. [CrossRef]

19.　Dominguez, J.M.; Hernandez, J.L.; Sandoval, G. Surface and catalytic properties of Al_2O_3–ZrO_2, solid solutions prepared by sol–gel methods. *Appl. Catal. A-Gen.* **2000**, *197*, 119–130. [CrossRef]

20.　Liu, P.J.; Wei, H.Z.; He, S.B.; Sun, C.L. Catalytic wet peroxide oxidation of m-cresol over Fe/gamma-Al_2O_3 and Fe-Ce/gamma-Al_2O_3. *Chem. Pap.* **2015**, *69*, 827–838. [CrossRef]

21.　Jongsomjit, B.; Panpranot, J.; Goodwin, J.G. Effect of zirconia-modified alumina on the properties of Co/γ-Al_2O_3 catalysts. *J. Catal.* **2003**, *215*, 66–77. [CrossRef]

22.　Guzman, J.; Carrettin, S.; Corma, A. Spectroscopic evidence for the supply of reactive oxygen during CO oxidation catalyzed by gold supported on nanocrystalline CeO_2. *J. Am. Chem. Soc.* **2005**, *127*, 3286–3287. [CrossRef] [PubMed]

23.　Damyanova, S.; Pawelec, B.; Arishtirova, K.; Huerta, M.V.M.; Fierro, J.L.G. Study of the surface and redox properties of ceria–zirconia oxides. *Appl. Catal. A-Gen.* **2008**, *337*, 86–96. [CrossRef]

24.　Culberson, C.F. Improved conditions and new data for the identification of lichen products by a standardized thin-layer chromatographic method. *J. Chromatogr. A* **1972**, *72*, 113–125. [CrossRef]

25.　Tsai, W.T.; Lee, M.K.; Chang, J.H.; Su, T.Y.; Chang, Y.M. Characterization of bio-oil from induction-heating pyrolysis of food-processing sewage sludges using chromatographic analysis. *Bioresour. Technol.* **2009**, *100*, 2650–2654. [CrossRef]

26.　Adam, J.; Blazsó, M.; Mészáros, E.; Stocker, M.; Nilsen, M.H.; Bouzga, A.; Hustad, J.E.; Gronli, M.; Oye, G. Pyrolysis of biomass in the presence of Al-MCM-41 type catalysts. *Fuel* **2015**, *8*, 1494–1502. [CrossRef]

27.　Wang, W.L.; Li, X.P.; Ye, D.; Cai, L.P.; Sheldon, Q. Catalytic pyrolysis of larch sawdust for phenol-rich bio-oil using different catalysts. *Renew. Energy* **2018**, *270*, 529–536. [CrossRef]

28.　An, Y.; Tahmasebi, A.; Yu, J.L. Mechanism of synergy effect during microwave co-pyrolysis of biomass and lignite. *J. Anal. Appl. Pyrolysis* **2017**, *128*, 75–82. [CrossRef]

29.　Li, Z.H.; Bi, Z.H.; Yan, L.F. Two-step hydrogen transfer catalysis conversion of lignin to valuable small molecular compounds. *Green Process. Synth.* **2017**, *4*, 363–370. [CrossRef]

30. Kurnia, I.; Karnjanakom, S.; Bayu, A.; Yoshida, A.; Rizkiana, J.; Prakoso, T.; Abudula, A.; Guan, G.Q. In-situ catalytic upgrading of bio-oil derived from fast pyrolysis of lignin over high aluminum zeolites. *Fuel Process. Technol.* **2017**, *167*, 730–737. [CrossRef]

31. Bridgwater, A.V. Review of fast pyrolysis of biomass and product upgrading. *Biomass Bioenergy* **2012**, *38*, 68–94. [CrossRef]

32. Lee, S.; Lee, M.-G.; Park, J. Catalytic upgrading pyrolysis of pine sawdust for bio-oil with metal oxides. *J. Mater. Cycles Waste Manag.* **2018**, *20*, 1553–1561. [CrossRef]

33. Lu, Q.; Zhang, J.; Zhu, X. Corrosion properties of bio-oil and its emulsions with diesel. *Chin. Sci. Bull.* **2008**, *53*, 3726–3734. [CrossRef]

34. Pattiya, A.; Titiloye, J.O.; Bridgwater, A.V. Fast pyrolysis of cassava rhizome in the presence of catalysts. *J. Anal. Appl. Pyrolysis* **2008**, *81*, 72–79. [CrossRef]

35. Lu, Q.; Li, W.-Z.; Zhang, D.; Zhu, X.-F. Analytical pyrolysis-gas chromatography/mass spectrometry (Py-GC/MS) of sawdust with Al/SBA-15 catalysts. *J. Anal. Appl. Pyrolysis* **2009**, *84*, 131–138.

36. Witsuthammakul, A.; Sooknoi, T. Selective hydrodeoxygenation of bio-oil derived products: Ketones to olefins. *Catal. Sci. Technol.* **2015**, *5*, 3639–3648. [CrossRef]

37. Tong, X.; Ma, Y.; Li, Y. Biomass into chemicals: Conversion of sugars to furan derivatives by catalytic processes. *Appl. Catal. A-Gen.* **2010**, *385*, 1–13. [CrossRef]

38. Meier, D.; Faix, O. State of the art of applied fast pyrolysis of lignocellulosic materials—A review. *Bioresour. Technol.* **1999**, *68*, 71–77. [CrossRef]

39. Wang, J.; Zhang, B.; Zhong, Z.P.; Ding, K.; Deng, A.D.; Min, M.; Min, M.; Ruan, R. Catalytic fast co-pyrolysis of bamboo residual and waste lubricating oil over an ex-situ dual catalytic beds of MgO and HZSM-5: Analytical PY-GC/MS study. *Energy Convers. Manag.* **2017**, *139*, 222–231. [CrossRef]

40. Kaewpengkrow, P.; Atong, D.; Sricharoenchaikul, V. Catalytic upgrading of pyrolysis vapors from Jatropha wastes using alumina, zirconia and titania based catalysts. *Bioresour. Technol.* **2014**, *163*, 262–269. [CrossRef]

41. Mui, E.L.K.; Cheung, W.H.; Lee, V.K.C.; McKay, G. Compensation effect during the pyrolysis of tyres and bamboo. *Waste Manag.* **2010**, *30*, 821–830. [CrossRef] [PubMed]

42. Lou, R.; Wu, S.B.; Lv, G.J. Effect of conditions on fast pyrolysis of bamboo lignin. *J. Anal. Appl. Pyrolysis* **2010**, *89*, 191–196. [CrossRef]